Received: 21 February 2018 | Revised: 22 March 2018 | Accepted: 12 April 2018
DOI: 10.1002/ppap.201800036

FULL PAPER

PLASMA PROCESSES AND POLYMERS

Growth mechanisms of sulfur-rich plasma polymers: Binary gas mixtures versus single precursor

Evelyne Kasparek[1] | **Damien Thiry**[2] | **Jason R. Tavares**[3] | **Michael R. Wertheimer**[4] | **Rony Snyders**[2,5] | **Pierre-Luc Girard-Lauriault**[1]

[1] Plasma Processing Laboratory, Department of Chemical Engineering, McGill University, Montreal QC H3A 2B2, Canada

[2] Chimie des Interactions Plasma-Surfaces (ChIPS), CIRMAP, Université de Mons, Mons 7000, Belgium

[3] Photochemical Surface Engineering Laboratory, Department of Chemical Engineering, École Polytechnique de Montréal, Montréal QC H3C 3A7, Canada

[4] Groupe des couches minces (GCM) and Department of Engineering Physics, École Polytechnique de Montréal, Montréal QC H3C 3A7, Canada

[5] Materia Nova Research Center, Parc Initialis, Mons 7000, Belgium

Correspondence
Pierre-Luc Girard-Lauriault, Plasma Processing Laboratory, Department of Chemical Engineering, McGill University, Montreal QC H3A 2B2, Canada.
Email: pierre-luc.girard-lauriault@mcgill.ca

Funding information
McGill University (MEDA, GMA); Fonds de recherche du Québec en nature et technologies (FRQNT) via Plasma-Québec; Natural Sciences and Engineering Research Council of Canada (NSERC); Canadian Foundation for Innovation (CFI); Région Wallonne

Thiol (SH)-terminated surfaces have gained interest over the past years due to their potential applications, especially in the biomedical field. In this work, SH-terminated films have been prepared by "co-polymerizing" gas mixtures of acetylene (C_2H_2) and hydrogen sulfide (H_2S) using low-pressure r.f. plasma-enhanced chemical vapor deposition. R.f. power greatly influences the deposition rate, sulfur content, [S], and thiol concentration, [SH], of the films, as confirmed by XPS (both before and after chemical derivatization), FTIR, and mass spectrometry measurements. These data are compared with those obtained in a similar discharge by using a single molecule precursor, propanethiol. Among other differences, it is demonstrated that [SH] is higher when using binary gas mixtures compared to the single molecule precursor.

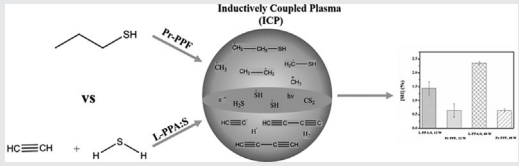

KEYWORDS
mass spectrometry, plasma polymerization, stability, sulfur-rich organic films, thiol derivatization

1 | INTRODUCTION

The development of thiol (SH)-functionalized surfaces is of great interest in surface modification and functionalization due to their increasing fields of applications, ranging from biomedicine to optics.[1] The presence of SH groups on surfaces allows for further functionalization via reaction with electron-rich-enes, alkynes, electron-deficient-enes, epoxies, and halogens, generating a "chemical toolbox" that offers a large variety of functional moieties for rapid manipulation of surface properties.[1g,2] Especially in the biomedical field, SH-terminated surfaces can be used for thiol-based coupling

reactions, where a series of (bio) molecules (e.g., biotin, DNA, proteins) are attached to the surfaces with retention of their biological activities.[3] Synthesis of surfaces supporting −SH groups through direct polymerization of monomers featuring these groups poses real challenges, as the thiol moiety is not tolerated in radical polymerization.[4] Therefore, SH-terminated surfaces have been synthesized using complex, multi-step wet-chemical approaches, often involving multiple different (toxic) solvents and long reaction times.[1d,1g,5]

In this context, low-pressure (LP) plasma deposition of plasma polymer films (PPFs) offers an alternative solvent-free, single-step, low reaction time, and environmental friendly process to synthesize SH-terminated surfaces. The properties of the resulting PPFs depend on different plasma process parameters such as absorbed power, P, pressure, p, precursor flow rate(s), F, mixture ratio, R, and precursor type. Two approaches are generally used to incorporate a desired functionality into PPFs, namely the use of (i) single molecule precursors, in which the desired functionality is already present; or (ii) binary gas mixtures comprising a hydrocarbon and a sulfur-based functional gas. In the specific case of −SH containing surfaces, allylmercaptan (AM)[1b,1c,6] and more recently propanethiol (Pr)[1e,7] are two examples of single molecule precursors that have been used. On the other hand, we have previously reported the use of binary gas mixtures of butadiene (C_4H_6) or ethylene (C_2H_4) and hydrogen sulfide (H_2S) to create SH-terminated PPF surfaces.[8] While the single molecule approach allows for direct incorporation of the functionalities into PPFs, the use of binary mixtures has been demonstrated to be at least equal, if not superior, in terms of functional group density and stability[9] (e.g., for the case of nitrogen (N)-containing coatings). The controllable gas mixture ratio, R, allows for increased versatility to achieve coatings with tailored properties. In our previous study,[8] we were able to grow PPFs with adjustable surface-near sulfur concentrations, [S], ranging from 2 to 48 at%, presenting thiol concentrations, [SH], up to 3%; these films exhibited high stability in aqueous solution, making them ideal candidates for further use in biomedical applications. Nevertheless, despite their promising properties, only few studies have so far been dedicated to the full characterization and understanding of the growth of SH-terminated PPFs. In addition, all those works focused on single monomer discharge plasmas. Thiry et al.[7a–f] reported a complete study, combining plasma diagnostics and PPF synthesis, regarding the influence of different plasma parameters on the chemical properties of propanethiol plasma polymers (Pr-PPF) deposited in r.f. discharges. These same authors also developed a derivatization method allowing specific identification of SH groups and their concentrations, [SH].[7]

Given this background, the main purpose of the present research has been to gain better understanding of growth mechanisms of S-containing PPFs prepared from binary gas mixtures of acetylene (C_2H_2) and H_2S, correlating plasma-phase and surface phenomena. Varying R and $<P>$ (the mean absorbed power per cycle, see Section 2.1), the plasma chemistry is examined by residual gas analysis (RGA) mass spectrometry, and these data are correlated with chemical composition of the PPFs using X-ray Photoelectron Spectroscopy (XPS) and Fourier Transform Infrared Spectroscopy (FTIR), along with PPF deposition kinetics. In addition, these data are compared with those for single precursor Pr-PPF counterparts.

2 | EXPERIMENTAL SECTION

2.1 | Thin film deposition and characterization

The experimental setup (Figure 1) consisted of a cylindrical stainless steel vacuum chamber (65 cm in length and 35 cm in diameter), evacuated by combined turbo-molecular and primary pumps to a base pressure, $p < 2*10^{-6}$ Torr. The power was applied using a single-turn copper coil (10 cm diameter) connected to an Advanced Energy 13.56 MHz r.f. power supply (CESAR 1310). The operating pressure during depositions was maintained at $p = 80$ mTorr by a throttle valve connected through a capacitive gauge (both from Nor-Cal Products). The flow rate of the hydrocarbon C_2H_2 (99%, Air Liquide), $F_{(C2H2)}$, was kept constant at 30 sccm, while that of H_2S (99%, Air Liquide), $F_{(H2S)}$, was varied between 0 and 30 sccm; this yielded values of R ($=F_{(H2S)}/F_{(C2H2)}$) ranging from 0 to 1. The flow rate of 1-propanethiol (99%, Sigma–Aldrich, the single molecule precursor), $F_{(Pr)}$, was fixed at 50 sccm, so as to maintain essentially the same total F, as in the gas mixture experiments where the elemental feed ratio ($X \equiv$ S/C = 1/3) was identical (i.e., for $R = 0.66$ in the gas mixture). The PPFs, henceforth designated "L-PPA:S" (for "low-pressure plasma-polymerized, sulfurized acetylene") or

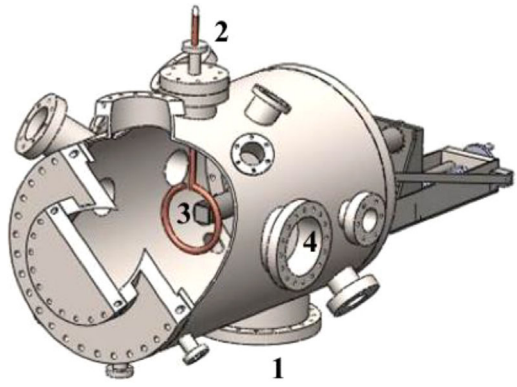

FIGURE 1 3D view of the plasma reactor: (1) Pumping line, (2) Water-cooled RF copper coil, (3) Substrate holder, (4) Mass spectrometer inlet port

"Pr-PPF" (for "propanethiol plasma polymer") were deposited on 500 μm-thick silicon wafers (Si-Mat) using pulsed plasma polymerization. The (nominal) value of mean power, $<P>$, absorbed in the plasma was modulated by varying the duty cycle, Δ; the relationship between the plasma "on" time and the pulse period, is shown in Equations (1) and (2), where P_{peak} is input power during the plasma "on" time.

$$< P >= P_{\text{Peak}}\Delta \quad (1)$$

$$\Delta = \frac{t_{on}}{t_{on} + t_{off}} \quad (2)$$

Table 1 summarizes the electrical power conditions used.

All PPF deposits were characterized by X-ray photoelectron spectroscopy (XPS), performed in a PHI 500 VersaProbe instrument (Physical Electronics), using monochromatic Al Kα radiation ($h\nu = 1486.6$ eV). The elemental composition (in atomic %, at. %) and the chemical environment of the elements were obtained by survey- and high-resolution, HR spectra, respectively. The former were acquired at a pass energy of 117.4 eV, a dwell time of 50 ms and energy steps of 1 eV, the latter at pass energy of 23.5 eV, dwell time of 50 ms and energy steps of 0.2 eV. Spectra were obtained at 45° emission angles; possible charging was corrected by referencing all peaks to the C1s peak at binding energy (BE) = 285.0 eV. The constituent elements were quantified from survey spectra using 2.3.16 PR 1.6 Casa XPS software, by integrating the areas under relevant peaks after a Shirley-type background subtraction.

Fourier-transform infrared (FTIR) spectroscopy (Bruker IFS 66V/S) was used for further chemical characterization. PPFs (≈200 nm thick) were deposited on KBr pellets and spectra (average of 32) were obtained within a spectral range from 4000 to 600 cm^{-1} in transmission mode at a resolution of 4 cm^{-1}. A blank KBr pellet served to acquire background spectra.

To quantify thiol concentrations, (SH), chemical derivatization with *N*-ethylmaleimide (99%, Sigma–Aldrich) was used, as recently described by Thiry et al.[7e] The reaction mechanism is shown in Scheme 1, where *N*-ethylmaleimide reacts selectively with SH via nucleophilic addition between the S atom and the double bond in the maleimide structure (thiol-ene click reaction), forming a stable thio-ether bond. The thiol-maleimide reaction offers several benefits, including high selectivity in the presence of multiple functional groups, rapid and quantitative conversion at low concentrations, and high stability in aqueous environments.[1g]

TABLE 1 Electrical conditions used in the present study

$<P>$ [W]	P_{peak} [W]	Δ [%]	t_{on} [ms]	t_{off} [ms]
12	120	10	0.2	1.8
48	120	40	0.8	1.2

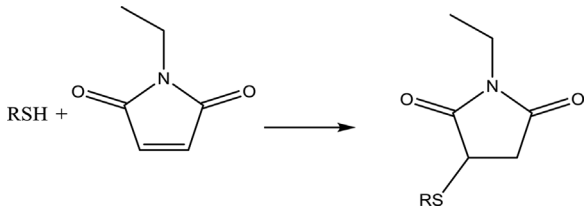

SCHEME 1 Derivatization reaction between a thiol group and *N*-ethylmaleimide

Typically, the derivatization reaction was carried out in phosphate buffer (KH_2PO_4/Na_2HPO_4, Chem Lab) solution at pH = 7, the *N*-ethylmaleimide concentration being fixed at 0.1 M. The samples were immersed in this solution for 78 h, following which they were rinsed in clean solution for 5 min to eliminate any unreacted molecules, then dried under a flow of dry nitrogen. XPS survey spectra were obtained before and after derivatization, allowing nitrogen, [N], and carbon, [C], concentrations to be quantified; [SH], was then calculated as follows:

$$[\text{SH}] = \frac{[\text{N}]}{[\text{C}] - 6[\text{N}]} \times 100(\%) \quad (3)$$

Deposition rates were determined by measuring coating thickness, *T*, with a Dektak 150 mechanical profilometer (Veeco), using a diamond tip with 2.5 μm curvature radius and an applied force of 0.1 mN. The coatings' stability against dissolution was examined after immersion in Milli-Q water for 24 h, using the profilometer to measure possible changes in *T* (Δ*T*, in%) before and after immersion at three different points.

2.2 | Plasma characterization

Gas-phase species in the plasma were investigated using a quadrupole mass spectrometer, MS (model HAL EQP 1000, Hiden Analytical), connected to the chamber by a 100 μm extraction orifice located about 30 cm from the coil. Residual gas analysis (RGA) MS measurements involved neutral species entering the instrument, which were then ionized by electron impact (EI) with electrons of kinetic energy fixed at 20 eV so as to avoid excessive fragmentation.

3 | RESULTS AND DISCUSSION

3.1 | Deposition kinetics and composition of PPF coatings

Deposition rates, *r* (in nm/min), of the L-PPA:S films as a function of gas mixture ratio, *R*, for $<P> = 12$ and 48 W, show that *r* decreased with rising *R* in both cases (Figure 2), as also observed in previous experiments with ethylene (C_2H_4),

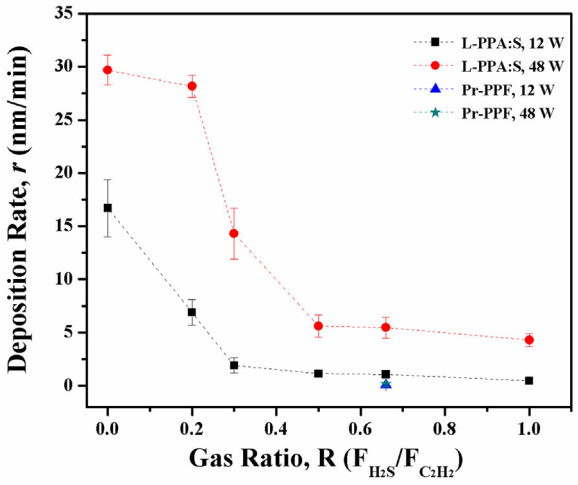

FIGURE 2 Deposition rates, *r*, of L-PPA:S films (squares, $<P> = 12$ W; circles, $<P> = 48$ W) as a function of gas mixture ratio, *R*, and of Pr-PPFs (triangle, $<P> = 12$ W; star, $<P> = 48$ W, overlapping here) at equivalent elemental feed ratio ($X = S/C = 1/3$). Error bars show standard deviations of three measurements. The lines are to guide the reader's eye

butadiene (C_4H_6), or C_2H_2 and N- or O-containing gas mixtures.[9b,9c,9e,9f,10]

This is due to the decreasing relative concentrations of C_xH_y radicals that create the PPFs' polymer-like backbone. Furthermore, with increasing *R*, more H_2S in the gas mixture gives rise to more of the highly reactive $H^{\bullet}$ and $S^{\bullet\bullet}$ radicals; the former can etch the growing film and thereby lead to a transition from radical-induced deposition to an ablation regime, thus the observed decrease in *r*.[9f] Similar behavior observed in the past for the case of N-rich films was also attributed to a threshold for the production of etching species.[11] Besides etching, quenching of radical species in the plasma, through recombination reactions, could also lead to a decrease in *r*. Indeed, radicals produced from H_2S dissociations (e.g., $H^{\bullet}$ and $S^{\bullet\bullet}$) could readily recombine with the ones formed from C_2H_2, thus reducing the availability of radicals for film deposition, leading to a decrease in deposition rate.

Note that at $<P> = 48$ W, L-PPA:S films showed significantly higher *r* values than at $<P> = 12$ W. Referring to Table 1, at $<P> = 48$ W the plasma "on" time was higher (0.8 vs. 0.2 ms), thereby leading to greater precursor fragmentation and higher concentration of film-forming species. Deposition rates of Pr-PPFs (Figure 2), prepared at the constant elemental feed rate ($X \equiv C/S = 1/3$) and total flow comparable to L-PPA:S films obtained at $R = 0.66$, revealed the same behavior, although significantly smaller, due to several reasons: (i) the saturated structure of propanethiol likely led to more dehydrogenation, which can induce increased etching; (ii) absence of unsaturations (i.e., double or triple bonds) in propanethiol, in contrast to C_2H_2, prevented uptake of unactivated precursor into the PPF; and (iii) mass spectrometry measurements (see Figure S1, Supporting Information) also showed very little fragmentation of the propanethiol precursor under the applied conditions, compared with previous results of Thiry et al.

For both $<P>$ values, [S] is seen to have increased monotonically with rising *R*, up to [S] ≈50 at. %, tending to plateau for $R > 0.66$ (Figure 3). Similar behavior was also observed in our previous work, where [S] up to ≈48 at. % was obtained with C_2H_4 as the hydrocarbon feed gas.[8] Lower [S] values at high $<P>$ can presumably be attributed to higher fragmentation, leading to many small volatile S-rich stable molecules that were pumped out of the chamber and did not contribute to film growth;[7d,7f,12] the higher the fragmentation, the less S-containing moieties might then be available for incorporation into the growing films. Similar trends for [S] were observed for Pr-PPFs, namely higher [S] was obtained at lower $<P>$ (more details under Section 3.3). These data also reveal a major difference when comparing with N- or O-based PPFs: especially at low $<P>$, [S] significantly exceeded that element's concentration in the feed gas mixture or in the precursor, an observation that was also reported when using propanethiol and attributed to trapped H_2S in the plasma polymer network.[7d,13] A major advantage of binary gas mixtures over a single molecule precursor is the following: Figure 3 and previous studies[8,9e,9f,10b,14] all showed that heteroelement concentration, [X] (here: [S]), can be controlled over a remarkably wide range (here: 10 at. % < [S] < 50 at. %). This flexibility evidently opens the use of these PPFs for numerous applications where a particular [X] value is

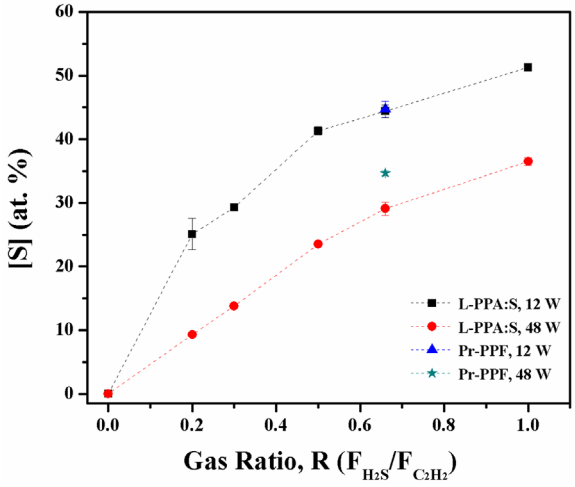

FIGURE 3 Sulfur concentrations, [S] (in at. %), as measured by XPS for L-PPA:S films (squares, $<P> = 12$ W; circles, $<P> = 48$ W) as a function of gas mixture ratio, *R*, and of Pr-PPFs (triangle, $<P> = 12$ W; star, $<P> = 48$ W) at equivalent elemental feed ratio ($X = S/C = 1/3$). Error bars show standard deviations of three measurements. The lines are to guide the reader's eye

required, for example, to select a specific value of refractive index.[1e]

Due to the complexity of plasma-chemical reactions, a large variety of S-containing groups are created, but the measured [S] value does not reveal whether it occurs as the SH-groups desired, for example, in biomedical applications. Indeed, S can exist in different allotropes (S—S—S, C—S—C, C—SH, ...), but these cannot readily be identified by XPS because different types of S-bonding do not result in appreciable chemical shifts, neither in the S2p nor in C1s HR-XPS spectra.[15] Therefore, in order to measure (SH) in L-PPA:S and Pr-PPFs, the selective and quantitative chemical derivatization reaction based on *N*-ethylmaleimide as labelling molecule was used.[7e] Figure 4 plots [SH] as a function of R at two different $<P>$ values, with FTIR measurements confirming the presence of these thiol moieties (see Figure S2, Supporting Information).

For $R < 0.5$ and $<P> = 48$ W it was not possible to measure [SH] of L-PPA:S films because the coatings cracked during derivatization, likely due to high internal stress caused by the higher power and carbon content.[16] At lower $<P>$, [SH] was seen to be nearly constant up to $R = 0.66$, ≈1–1.7%, within experimental error, while the value dropped with further increase in R. At the higher $<P>$, [SH] increased with rising R, up to about 3.4%. Therefore, even if [S] was overall lower at higher $<P>$, deposits of greater quality (higher [SH]) were obtained. Contrary to propanethiol, where higher fragmentation resulted in lower thiol retention,[7f,17] in the case of gas mixtures fragmentation was needed to create that desired chemical functionality. At higher $<P>$, higher fragmentation led to more of such active thiol-forming species, hence to the observed increasing [SH] values. Similar observations were reported by Buddhadasa et al.[9g] for the case of ammonia/butadiene feed-gas mixtures, where the concentration of amino groups, [NH2], was found to increase with rising P.

[SH] (≈0.6%) of Pr-PPFs was apparently not affected by $<P>$, as previously observed for other electrical and pressure conditions,[7f] being significantly lower than for L-PPA:S ([SH] ≈1.5 and ≈2.5%). The use of binary mixtures was therefore advantageous for higher thiol incorporation. At this stage, the exact mechanism(s) remain elusive and require further experiments over wider parameter ranges.

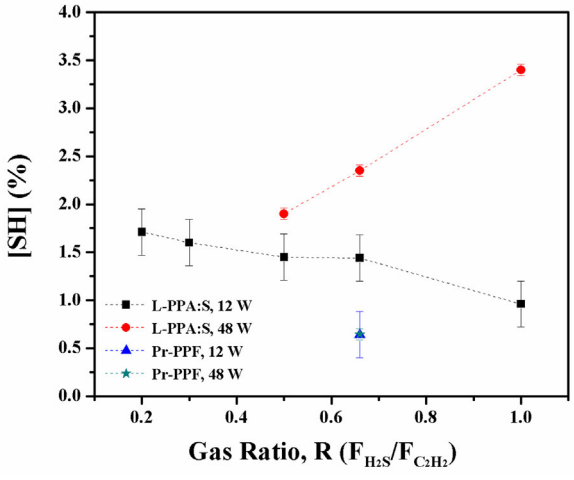

FIGURE 4 Proportion of carbon bearing the −SH group, [SH] (in %), determined using chemical derivatization XPS of L-PPA:S films (squares, $<P> = 12$ W; circles, $<P> = 48$ W), as a function of gas mixture ratio, R, and of Pr-PPFs (triangle, $<P> = 12$ W; star, $<P> = 48$ W, overlapping here) at equivalent elemental feed ratio ($X = S/C = 1/3$). Error bars show standard deviations of three measurements. The lines are to guide the reader's eye

3.2 | Ageing in water and in air

The stability of PPFs in water and in air is of crucial importance for potential biomedical applications, for example. For the case of N- and O-rich PPF coatings, stability has already been extensively discussed:[9a,9b,18] high concentrations of heteroatoms (N or O) lead to higher solubility in polar solvents (e.g., water) and a higher instability in air, commonly referred to as "ageing." This is attributed, among other factors, to the presence of soluble low molecular weight (LMW) fractions formed during deposition, which are extractable in polar solvents, and to oxidation of dangling bonds and degradation of unstable functional groups in contact with air.[9a,9b,10a,12b,14,19] In the specific case of sulfur-based coatings, Thiry et al[13] showed that S-containing species (e.g., H_2S) were trapped in the PPF matrix and released after immersion in water. Therefore, S/C ratios of our coatings were measured before and after immersion in *N*-ethylmaleimide solution (Figure 5). Except for the $<P> = 48$ W/$R = 1$ sample, conditions under which many stable molecules were created (see Section 3.3), little reduction in S/C was observed after immersion; this suggests that a small proportion of S-containing molecules were trapped in the PPF matrix and/or that the degree of chemical bonding was sufficient to prevent release of such possibly trapped molecules during immersion.

To complete this part of the study, possible thickness loss after immersion in Milli-Q water during 24 h was also examined, as extensively reported in the literature for several other families of plasma polymers.[8,9f,18b,19b,20] Similar to the case of C_4H_6- and C_2H_4-based PPF coatings, the present L-PPA:S films were found to be largely insoluble in Milli-Q water, for $0 \le R \le 1$: the largest observed values of $\Delta T/T$ were about 20% (positive or negative), comparable to the cumulative measurement uncertainty (see Figure S3, Supporting Information). Pr-PPFs deposited at $<P> = 12$ W showed similar stability to the corresponding L-PPA:S films while for $<P> = 48$ W, a higher solubility was observed

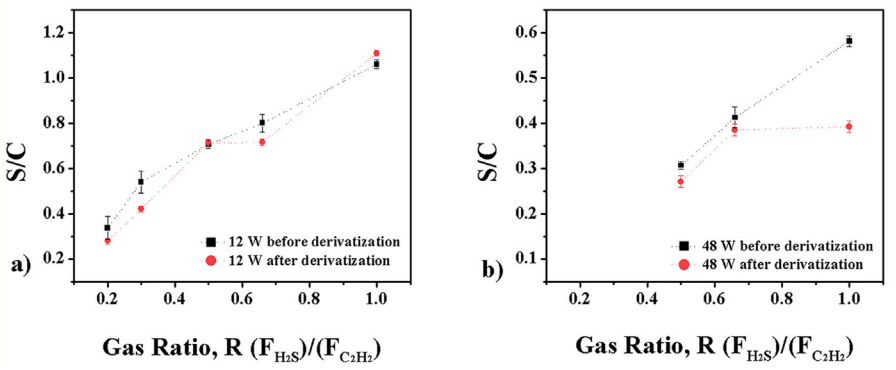

FIGURE 5 S/C ratios measured by XPS before (squares) and after (circles) immersion in *N*-ethylmaleimide solution: a) L-PPA:S films obtained at $<P> = 12$ W, and b) at $<P> = 48$ W, as a function of gas mixture ratio, *R*. Error bars show standard deviations of three measurements. The lines are to guide the reader's eye

(≈25% loss of thickness, see Figure S3, Supporting Information). A possible explanation for their stability might be that these coatings were particularly highly cross-linked on account of acetylene's triple bond, as also reported for L-PPA:N films.[9f]

To complete the study of ageing, surface-near oxygen concentrations, [O], of the L-PPA:S films were measured by XPS as a function of *R* after storing them in ambient air for 3 days.

Figure 6 shows that [O] decreased with rising R for both values of $<P>$. As already discussed, increasing *R* decreased the concentration of C_xH_y radicals in the plasma, hence that of C-centered radicals in the coatings (as opposed to S-bearing groups). Figure 5 clearly revealed proportional rise of S/C with increasing *R*; as atmospheric oxygen presumably only reacted with C-centered radicals, the drop in [O] noted in Figure 6 therefore stands to reason.[21]

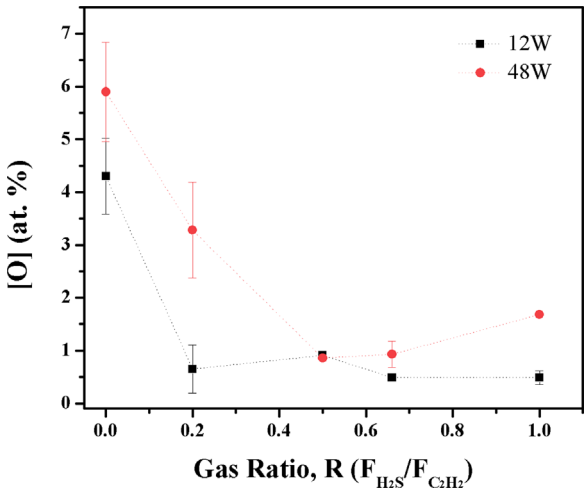

FIGURE 6 Surface-near oxygen concentrations, [O] (in at. %, obtained by XPS) as a function of gas mixture ratio, *R*, of L-PPA:S films (squares, $<P> = 12$ W; circles, $<P> = 48$ W) stored for 3 days in ambient air. Error bars show standard deviations of three measurements. The lines are to guide the reader's eye

3.3 | Mass-spectrometry measurements

To better understand growth mechanisms of L-PPA:S films, plasma chemistry of the gas mixtures was examined by mass spectrometry measurements using residual gas analysis (RGA). Mass spectra of the precursor gases (Figure 7a,b) revealed peaks at m/z = 26 for C_2H_2 and m/z = 34 for H_2S in the absence of plasma. Additional peaks in Figure 7a can presumably be assigned to slight impurities in C_2H_2.[22]

Plasma ignition led to changes in concentrations and to the production of new species, depending on *R* and $<P>$ (Figure 7c,d). All peaks in the mass spectra are identified in Table 2.

At $R = 0$, a quite intense peak at m/z = 50 corresponding to C_4H_2 was detected. As *R* increased (more H_2S was present in the gas mixture), an additional peak corresponding to CS_2 appeared at m/z = 76, which increased in amplitude with rising *R* and $<P>$, whereas that corresponding to C_4H_2 decreased. The abundance of CS_2 points to reactions between feed gas species in the plasma; on the other hand, earlier studies showed little evidence of such reactions between ammonia and the hydrocarbon.[9g] However, etching reactions can apparently also contribute to formation of CS_2: when a pure H_2S discharge was ignited at $<P> = 48$ W (Figure 7f), the m/z = 76 peak revealed that etching of PPF coatings on the chamber walls must have taken place. Those etching reactions also contributed to the drop in *r*, as previously evoked. CS_2 production in S-containing discharges had already been reported for propanethiol,[7d,7f] methanethiol,[23] and thiophene plasmas. Here, the creation of CS_2 can mainly be attributed to gas phase reactions between C_2H_2 and H_2S in the plasma, because its peak at m/z = 76 was much higher than that corresponding to etching reactions.

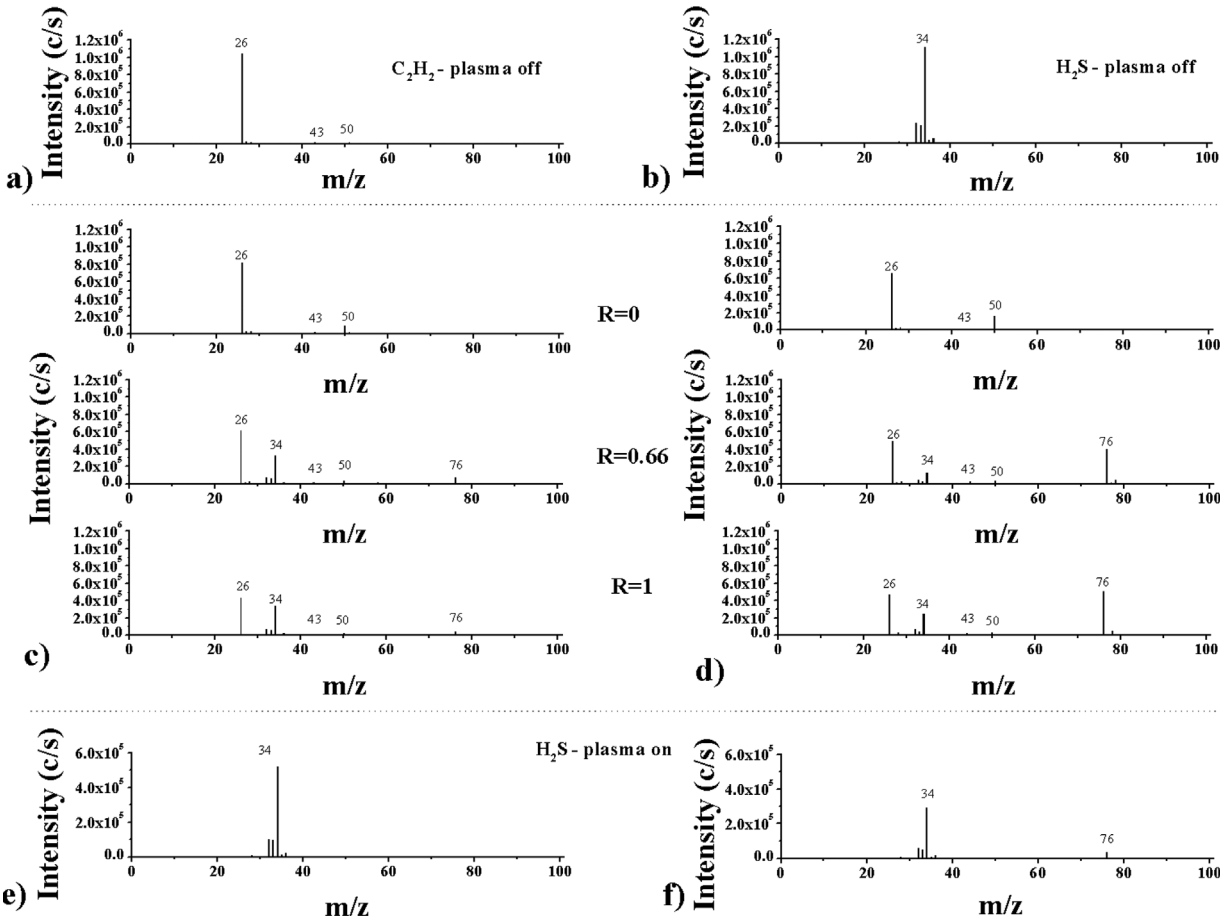

FIGURE 7 Mass spectra of (a) C_2H_2 and (b) H_2S at plasma "off" conditions (spectra show no significant fragmentation of the pure gases in the ionisation source of the spectrometer); of three different $C_2H_2 + H_2S$ mixtures ($R = 0$, $R = 0.66$, and $R = 1$) in plasmas sustained at (c) $<P> = 12$ W and (d) $<P> = 48$ W; and mass spectra of pure H_2S plasmas sustained at (e) $<P> = 12$ W and (f) $<P> = 48$ W (Note; creation of CS_2, m/z = 76, was observed at $<P> = 48$ W only)

Lower-mass fragments detected in previous work, especially in acetylene plasmas (e.g. H_2, $H^\bullet$, and $C_2H^\bullet$), were not noted here to any appreciable extent.[22,24] This may have been due to a lower detection limit of the mass spectrometer, but also to the high sticking coefficient, β, of $C_2H^\bullet$ ($\beta = 0.9$),[24] which rendered detection of this radical particularly challenging: It has been recognized as the major contributor to *a*-C:H film growth in pure acetylene plasmas.[22,24–25]

In order to connect mass spectrometry results with L-PPA:S film characteristics, we examined the extent of fragmentation of both precursors, α, as a function of R at different $<P>$ (Figure 8), according to Equation (4):

$$\alpha = I_{\mathrm{rel}}(m)_{\mathrm{on}} - I_{\mathrm{rel}}(m)_{\mathrm{off}} \tag{4}$$

where $I_{\mathrm{rel}}(m)_{\mathrm{on}}$ and $I_{\mathrm{rel}}(m)_{\mathrm{off}}$ are the relative peak intensities of precursor (m) when the plasma is "on" and "off," respectively. The relative abundance of mass m species, $I_{\mathrm{rel}}(m)$, in the plasma is then defined as:

$$I_{\mathrm{rel}}(m) = \frac{I(m)}{\Sigma_{\mathrm{m}} I(m)} \tag{5}$$

where $I(m)$ are the experimentally observed values recorded in the mass spectra of mass m, respectively.

Based on Equation (4), negative α values indicate decreased peak intensity, thus higher fragmentation of the precursors; the more negative, the higher the extent of fragmentation in the plasma. Some fragmentation was observed at all values of R, although little at low $<P>$ for

TABLE 2 Attribution of peaks observed in the various mass spectra, Figure 7 (a-f)

m/z	Ions
25–28	$[C_2H_\chi]^+$ $\chi = 1$–4
32–34	$[H_\chi S]^+$ $\chi = 0$–2
76	$[CS_2]^+$

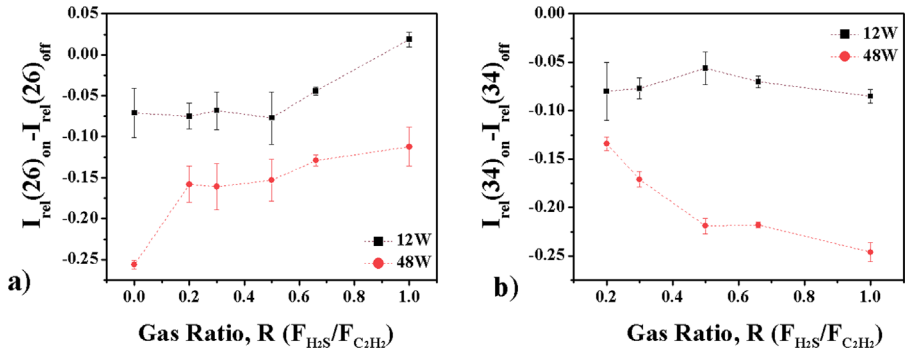

FIGURE 8 Extent of fragmentation, α, for (a) C_2H_2 and (b) H_2S (squares, $<P> = 12$ W; circles, $<P> = 48$ W) as a function of gas mixture ratio, *R*. Error bars show standard deviations of three measurements. The lines are to guide the reader's eye

C_2H_2; for H_2S, increased fragmentation was observed with rising *R*, especially at the higher $<P>$. Indeed, for both gases, fragmentation was higher at $<P> = 48$ W, confirming the assumptions reported in Section 3.1: the precursors were exposed to the plasma for a longer period of time, thereby increasing the probability of collisions with energetic electrons. This led to higher fragmentation and it can explain the observed larger values of *r*, lower [S] and higher [SH]. Nevertheless, decreased [S] and increased [SH] cannot readily be explained solely by higher precursor fragmentation. We therefore also focused on the evolution of other important species, such as CS_2 (m/z = 76) (Figure 9).

Lower amounts of CS_2 at $<P> = 12$ W could be directly observed in the mass spectra (Figure 7c) and correlated with a lower extent of precursor fragmentation (Figure 8); at $<P> = 48$ W, fragmentation was high, giving rise to increasing production of CS_2 with rising *R*, up to saturation for $R > 0.66$, probably due to insufficient numbers of C_xH_y radicals. The concentration of CS_2 in the discharge correlates inversely with [S] in the PPFs:[7d] increased CS_2 production at high $<P>$ could therefore help explain the reduced amount of sulfur available for incorporation into the growing films, hence the observed lower [S] values than at lower $<P>$ (Figure 3).

To help better understand the evolution of [SH] with rising *R* (Figure 4), we next focused on fragments that could possibly insert −SH moieties into the growing L-PPA:S films, namely SH (m/z = 33) and $S^{\bullet\bullet}$ (m/z = 32). Both of these already being observed in the absence of plasma (Figure 7b), Equation (6) takes into account fragments produced in the ionization source of the mass spectrometer by electron impact:[17b]

$$I_c(m) = \frac{\left(I(m)_{on} - \left(I(m)_{off} \cdot \frac{I(34)_{on}}{I(34)_{off}}\right)\right)}{\Sigma_m I(m)} \qquad (6)$$

where $I_c(m)$ is the corrected intensity of mass *m* (here either 33 or 32), and $I(m)_{on}$ and $I(m)_{off}$ are the experimentally observed peak intensities for mass *m* when the plasma is on and off, respectively; I(34) is the peak intensity corresponding to the H_2S precursor gas.

$I_c(33)$ is seen to have increased with rising *R*, reaching a maximum near $R = 0.66$ (Figure 10a). Furthermore, for similar *R* values, the relative amount of $SH^{\bullet}$ was higher at $<P> = 12$ W. Figure 4 depicts a rather different trend in (SH) than the one shown here, namely a monotonic decrease with rising *R*. This would imply that $SH^{\bullet}$ radicals were not directly responsible for SH-groups in L-PPA:S films. Now examining Figure 10b), the atomic $S^{\bullet\bullet}$peak (m/z = 32) was also seen to increase with rising *R* for both $<P>$ values, reaching maxima at $R = 0.66$. However, contrary to $SH^{\bullet}$ (Figure 10a), the creation of $S^{\bullet\bullet}$ was greater at the higher $<P>$, presumably on account of multistep fragmentation (i.e., $H_2S \rightarrow SH^{\bullet} \rightarrow S^{\bullet\bullet}$). This would indeed be favored at high $<P>$ due to longer exposure time in the plasma, which in turn might help explain

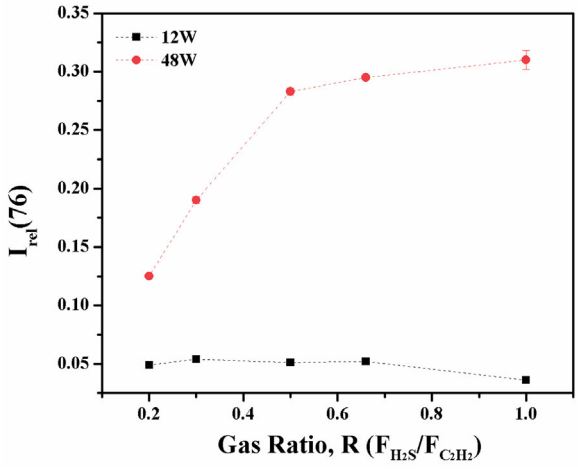

FIGURE 9 Plot of $I_{rel}(76)$ (squares, $<P> = 12$ W; circles, $<P> = 48$ W) as a function of gas mixture ratio, *R*. Error bars show standard deviations of three measurements. The lines are to guide the reader's eye

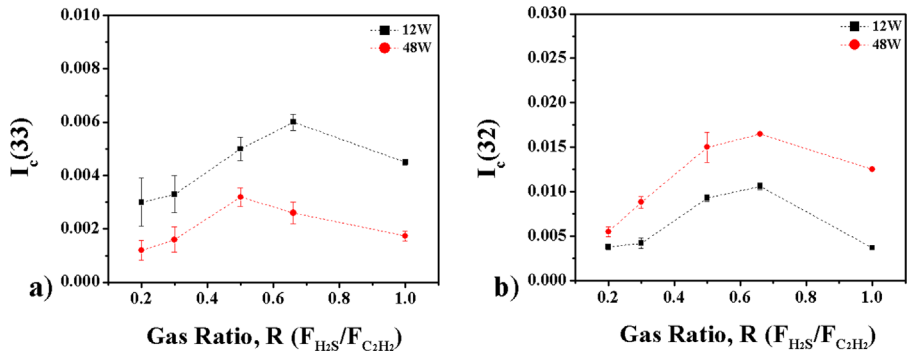

FIGURE 10 Evolution of species that could lead to SH-groups in L-PPA:S films (a) $SH^{\bullet}$ and (b) $S^{\bullet\bullet}$(squares, $<P> = 12$ W; circles, $<P> = 48$ W) as a function of gas mixture ratio, R. Error bars show standard deviations of three measurements. The lines are to guide the reader's eye

the increased formation of CS_2. Considering that larger amounts of atomic hydrogen were available at higher $<P>$ with rising R (see Figure 8), the incorporation of $S^{\bullet\bullet}$ and accompanying formation of −SH groups in growing L-PPA:S films would therefore be favored, as indeed observed in Figure 4.

Summarizing, knowledge of the plasma composition from mass spectrometry measurements enables a better understanding of deposition kinetics and film composition (at least in terms of [S]); however, the evolution of [SH] cannot yet be fully explained by gas phase reactions only. Theoretical calculations could help in predicting different fragmentation pathways as a function of the employed plasma paramaters and thus give a better understanding for the evolution of [SH], as was previously done for a propanethiol plasma.[7d,7f]

4 | DISCUSSION AND CONCLUSIONS

The chemistry and growth mechanisms of plasma-assisted deposition from single-molecule precursors have been extensively studied in the past, relating to the fabrication and characterization of amine-, hydroxyl- and/or carboxyl-, and thiol(SH)-rich plasma-polymer films. However, no such studies have been reported for the case of feed-gas mixtures leading to SH-terminated films, conducted by the present authors. Here, we have aimed to gain deeper knowledge of the chemistry involving a new family of SH-containing films, namely acetylene-based sulfur-rich ones (L-PPA:S), created by "co-polymerizing" mixtures of a hydrocarbon (here C_2H_2) and H_2S by low-pressure r.f plasma polymerization. The impact of varying gas mixture ratio, R, and applied power, $<P>$, was investigated by way of surface- (XPS and FTIR) and plasma-related (MS) analyses.

Deposition rates, r, of L-PPA:S coatings as a function of R followed the same trends for both $<P>$ values of investigated, higher $<P>$ leading to higher r values. This could be correlated with more pronounced precursor fragmentation at higher $<P>$, as also confirmed by MS measurements. Sulfur concentrations, [S], in the films increased monotonically with rising R, up to [S] ≈50 at. % at $<P> = 12$ W, while higher $<P>$ led to a decrease in [S]. This was attributed to intense precursor fragmentation that resulted in the production of many S-rich stable molecules, which did not appreciably contribute to film growth and were pumped out of the chamber. This was also confirmed by MS measurements, namely increased production of CS_2 at higher $<P>$. Somewhat surprisingly, higher thiol concentrations, [SH], were found to occur in the higher $<P>$ L-PPA:S films. Contrary to the case of a single molecule precursor, extensive precursor-gas fragmentation is first needed to produce the desired functionality(ies), here [SH], when using binary gas mixture. Therefore, [SH] increase at higher $<P>$ is again correlated with the higher extent of precursor fragmentation under these conditions. Nevertheless, MS measurements revealed that $SH^{\bullet}$ in the gas phase was not alone responsible for [SH] in the films, but that other surface reactions need to be considered in addition.

Comparison with Pr-PPF films prepared using the single-molecule precursor, propanethiol, with a constant S/C ratio (=1/3), revealed comparable [S], but lower r and [SH] values than those obtained for the case of L-PPA:S films. This is surprising because the propanethiol molecule already possesses the thiol functionality, which ought to lead to higher [SH]; this had so far been considered an advantage of the single molecule approach over the use of gas mixture.

In conclusion, binary gas mixtures offer (i) excellent control of [S] over a wide range (here: 10 at. % < [S] <50 at. %); (ii) flexibility over the desired [S] due to the ability to readily vary and control R; (iii) higher retention of thiol functionalities in the films; and (iv) excellent stability towards dissolution in aqueous media and ageing in air. All of these mentioned advantages together render L-PPA:S films superior candidates for applications, for example, biomedical ones.

ACKNOWLEDGMENTS

The authors gratefully acknowledge financial support from McGill University (MEDA, GMA), from the Fonds de recherche du Québec en nature et technologies (FRQNT) via Plasma-Québec; from the Natural Sciences and Engineering Research Council of Canada (NSERC), and the Canadian Foundation for Innovation (CFI). D. Thiry thanks the "Région Wallonne" for financial support through the Cleanair project.

ORCID

Evelyne Kasparek http://orcid.org/0000-0002-9406-5627
Damien Thiry http://orcid.org/0000-0001-6703-1512
Jason R. Tavares http://orcid.org/0000-0002-3828-2993

REFERENCES

[1] a)A. Niklewski, W. Azzam, T. Strunskus, R. Fischer, C. Wöll, *Langmuir* **2004**, *20*, 20; b)L. Harris, W. Schofield, K. Doores, B. Davis, J. Badyal, *J. Am. Chem. Soc*. **2009**, *131*, 22; c)W. Schofield, J. McGettrick, T. Bradley, J. Badyal, S. Przyborski, *J. Am. Chem. Soc*. **2006**, *128*, 7; d)D. Weinrich, P. C. Lin, P. Jonkheijm, U. T. Nguyen, H. Schroder, C. M. Niemeyer, K. Alexandrov, R. Goody, H. Waldmann, *Angew. Chem. Int. Ed. Engl*. **2010**, *49*, 7; e)F. J. Aparicio, D. Thiry, P. Laha, R. Snyders, *Plasma Process. Polym*. **2016**, *13*, 8; f)S. D. Bhagat, J. Chatterjee, B. Chen, A. E. Stiegman, *Macromolecules* **2012**, *45*, 3; g)A. B. Lowe, C. N. Bowman, **2013**.

[2] W. J. Yang, K.-G. Neoh, E.-T. Kang, S.L. -M. Teo, D. Rittschof, *Polym. Chem*. **2013**, *4*, 10.

[3] a)S. Chen, L. M. Smith, *Langmuir* **2009**, *25*, 20; b)M. A. C. Campos, J. M. J. Paulusse, H. Zuilhof, *Chem. Commun*. **2010**, *46*, 30;

[4] D. Liu, D. J. Broer, *Responsive Polymer Surfaces: Dynamics in Surface Topography*. John Wiley & Sons, **2017**.

[5] P. Jonkheijm, D. Weinrich, M. Köhn, H. Engelkamp, P. Christianen, J. Kuhlmann, J. C. Maan, D. Nüsse, H Schroeder, R. Wacker, *Angewandte Chemie* **2008**, *120*, 23.

[6] L. Harris, W Schofield, J. Badyal, *Chem. Mater*. **2007**, *19*, 7.

[7] a)D. Thiry, F. J. Aparicio, N. Britun, R. Snyders, *Surf. Coat. Technol*. **2014**, *241*; b)D. Thiry, N. Britun, S. Konstantinidis, J. P. Dauchot, L. Denis, R. Snyders, *Appl. Phys. Lett*. **2012**, *100*, 7; c)D. Thiry, N. Britun, S. Konstantinidis, J.-P. Dauchot, L. Denis, R. Snyders, *Appl. Phys. Lett*. **2012**, *100*, 7; d)D. Thiry, N. Britun, S. Konstantinidis, J.-P. Dauchot, M. Guillaume, J. R. M. Cornil, R. Snyders, *J. Phys. Chem. C* **2013**, *117*, 19; e)D. Thiry, R. Francq, D. Cossement, D. Guerin, D. Vuillaume, R. Snyders, *Langmuir* **2013**, *29*, 43; f)D. Thiry, R. Francq, D. Cossement, M. Guillaume, J. Cornil, R. Snyders, *Plasma Process. Polym*. **2014**, *11*, 6.

[8] E. Kasparek, J. R. Tavares, M. R. Wertheimer, P.-L. Girard-Lauriault, *Plasma Process. Polym*. **2016**, *13*, 9.

[9] a)J.-C. Ruiz, A. St-Georges-Robillard, C. Thérésy, S. Lerouge, M. R. Wertheimer, *Plasma Process. Polym*. **2010**, *7*, 9; b)F. Truica-Marasescu, J.-C. Ruiz, M. R. Wertheimer, *Plasma Process. Polym*. **2012**, *9*, 5; c)F. Truica-Marasescu, M. R. Wertheimer, *Macromol. Chem. Phys*. **2008**, *209*, 10; d)F. Truica-Marasescu, S. Pham, M. R. Wertheimer, *Nucl. Instrum. Methods Phys. Res. B* **2007**, *265*, 1; e) J.-C. Ruiz, P.-L. Girard-Lauriault, F. Truica-Marasescu, M. R. Wertheimer, *Radiat. Phys. Chem*. **2010**, *79*, 3; f)A. Contreras-Garcia, M. R. Wertheimer, *Plasma Chem. Plasma Process*. **2013**, *33*, 1; g)M. Buddhadasa, C. R. Vandenabeele, R. Snyders, P. L. Girard-Lauriault, *Plasma Process. Polym.*

[10] a)J. C. Ruiz, P. L. Girard-Lauriault, M. R. Wertheimer, *Plasma Process. Polym*. **2015**, *12*, 3; b)M. Buddhadasa, P.-L. Girard-Lauriault, *Thin Solid Films* **2015**, *591*.

[11] a)D. Hegemann, M.-M. Hossain, *Plasma Process. Polym*. **2005**, *2*, 7; b)F. Truica-Marasescu, P.-L. Girard-Lauriault, A. Lippitz, W. E. S. Unger, M. R. Wertheimer, *Thin Solid Films* **2008**, *516*, 21; c)M. M. Hossain, D. Hegemann, G. Fortunato, A. S. Herrmann, M. Heuberger, *Plasma Process. Polym*. **2007**, *4*, 4.

[12] a)L. Denis, F. Renaux, D. Cossement, C. Bittencourt, N. Tuccitto, A. Licciardello, M. Hecq, R. Snyders, *Plasma Process. Polym*. **2011**, *8*, 2; b)P. Rupper, M. Vandenbossche, L. Bernard, D. Hegemann, M. Heuberger, *Langmuir* **2017**, *33*, 9; c)D. Hegemann, E. Körner, N. Blanchard, M. Drabik, S. Guimond, *Appl. Phys. Lett*. **2012**, *101*, 21.

[13] D. Thiry, F. J. Aparicio, P. Laha, H. Terryn, R. Snyders, *J. Vac. Sci. Technol. A* **2014**, *32*, 5.

[14] F. Truica-Marasescu, M. R. Wertheimer, *Plasma Process. Polym*. **2008**, *5*, 1.

[15] a)J. A. Gardella Jr, S. A. Ferguson, R. L. Chin, *Appl. Spectrosc*. **1986**, *40*, 2; b)H. Peisert, T. Chassé, P. Streubel, A. Meisel, R. Szargan, *J. Electron. Spectros. Relat. Phenomena*. **1994**, *68*; c)M. Volmer, M. Stratmann, H. Viefhaus, *Surf. Interface Anal*. **1990**, *16*, 1.

[16] a)S. Vasquez, C. A. Achete, C. P. Borges, D. F. Franceschini, F. L. Freire, E. Zanghellini, *Diam. Relat. Mater*. **1997**, *6*, 5; b)G. A. Abbas, S. S. Roy, P. Papakonstantinou, J. A. McLaughlin, *Carbon* **2005**, *43*, 2; c)x Zajı, L. čková, S. Rudakowski, H. W. Becker, D. Meyer, M. Valtr, K. Wiesemann, *Thin Solid Films* **2003**, *425*, 1.

[17] a)K. S. Siow, L. Britcher, S. Kumar, H. J. Griesser, *Plasma Process. Polym*. **2006**, *3*, 6; b)D. Thiry, S. Konstantinidis, J. Cornil, R. Snyders, *Thin Solid Films* **2016**, *606*.

[18] a)M. Vandenbossche, D. Hegemann, *Curr. Opin. Solid State Mater. Sci*. **2018**; b)J.-C. Ruiz, P.-L. Girard-Lauriault, M. R. Wertheimer, *Plasma Process. Polym*. **2015**, *12*, 3.

[19] a)Z. Zhang, Q. Chen, W. Knoll, R Forch, *Surface Coat. Technol*. **2003**, *174*; b)K. Vasilev, L. Britcher, A. Casanal, H. J. Griesser, *J. Phys. Chem. B* **2008**, *112*, 35; c)F. Truica-Marasescu, P. Jedrzejowski, M. R. Wertheimer, *Plasma Process. Polym*. **2004**, *1*, 2.

[20] a)J. C. Ruiz, A. St-Georges-Robillard, C. Thérésy, S. Lerouge, M. R. Wertheimer, *Plasma Process. Polym*. **2010**, *7*, 9; b)D. Hegemann, B. Hanselmann, S. Guimond, G. Fortunato, M.-N. Giraud, A. G. Guex, *Surf. Coat. Technol*. **2014**, 255; c)A. Manakhov, L. Zajíčková, M. Eliáš, J. Čechal, J. Polčák, J. Hnilica, Š Bittnerová, D. Nečas, *Plasma Process. Polym*. **2014**, *11*, 6; d)D. Hegemann, B. Hanselmann, N. Blanchard, M. Amberg, *Contrib. Plasma Phys*. **2014**, *54*, 2; e)S. Lerouge, J. Barrette, J.-C. Ruiz, M. Sbai, H. Savoji, B. Saoudi, M. Gauthier, M. R. Wertheimer, *Plasma Process. Polym*. **2015**, *12*, 9.

[21] a)J. P. Booth, G. Cunge, P. Chabert, N. Sadeghi, *J. Appl. Phys*. **1999**, *85*, 6; b)M. J. Sowa, M. E. Littau, V. Pohray, J. L. Cecchi, *J. Vac. Sci. Technol*. **2000**, *18*, 5.

[22] J. Benedikt, *J. Phys. D Appl. Phys*. **2010**, *43*, 4.

[23] C.-H. Tsai, W.-J. Lee, C.-Y. Chen, P.-J. Tsai, G.-C. Fang, M. Shih, *Plasma Chem. Plasma Process*. **2003**, *23*, 1.

[24] A. Baby, C Mahony, P. Maguire, *Plasma Sources Sci. Technol.* **2011**, *20*, 1.
[25] J. R. Doyle, *J. Appl. Phys.* **1997**, *82*, 10.

SUPPORTING INFORMATION

Additional Supporting Information may be found online in the supporting information tab for this article.

How to cite this article: Kasparek E, Thiry D, Tavares JR, Wertheimer MR, Snyders R, Girard-Lauriault P-L. Growth mechanisms of sulfur-rich plasma polymers: Binary gas mixtures versus single precursor. *Plasma Process Polym.* 2018;15: e1800036. https://doi.org/10.1002/ppap.201800036